Superconductivity of graphenelike hydrogen in H$_2$He at high pressure

Kang Yang, Wenwen Cui ![ORCID],[*] Jian Hao, Jingming Shi ![ORCID], and Yinwei Li[†]

Laboratory of Quantum Functional Materials Design and Application, School of Physics and Electronic Engineering,
Jiangsu Normal University, Xuzhou 221116, China

The structural diversity of hydrogen under high pressure is crucial for understanding its physical properties, especially for the superconductivity. Here, a combination of crystal structure prediction and first-principle calculations has predicted a metastable H$_2$He at ultrahigh pressure of 800 GPa, where H atoms are arranged in graphenelike structure. H$_2$He shows weak superconductivity with critical temperature of 4 K, which significantly increases to 155 and 201 K at electron doping of 0.6 and 1.2 e, respectively. Analysis suggests that the enhanced superconductivity is closely associated with the graphenelike H sublattice. The doped electrons almost transfer to H sublattice, inducing the increased H-derived density of states at the Fermi level, as well as their coupling with the phonon modes of graphenelike H layers. The current results could stimulate the experiment to search for more diverse hydrogen species at high pressure and provide a feasible way to design high-T_c superconductors as well.

I. INTRODUCTION

Many efforts [1–5] have sought to find superconductors after Onnes firstly discovered superconductivity in 1911 [6]. The established microscopic mechanism for describing the conventional superconductivity is Bardeen-Cooper-Schrieffer (BCS) theory [7]. According to this theory, metallic hydrogen would exhibit great superconductivity due to high Debye temperature and the strong electron-phonon coupling [8–11], however, the experimental metallization of hydrogen remains a significant challenge [10,12,13], with a recent report claiming its synthesis at 495 GPa [14].

As an alternative, metallization could be achieved at much lower pressure in hydrogen-rich materials due to "chemical precompression" [15]. Of the many structural predictions for high-T_c compounds, some have been subsequently synthesized (e.g., H-S [16–18], LaH$_{10}$ [19–22], Y-H [23–27], Ce-H [28,29], and CaH$_6$ [30–32]). These hydrides have revealed several new structural units for hydrogen other than atomic H and molecular H$_2$: examples are H$_3$, H$_4$, H$_5$, H$_8$, H$_{10}$ [1], H$_{12}$ tube [33], and H cages [19,23,24,30,34,35]. Particularly promising are H-cage hydrides with extremely high predicted T_c : examples are 303 K in binary YH$_{10}$ (at 400 GPa) [19,23] and 473 K in ternary Li$_2$MgH$_{16}$ (at 300 GPa) [35]. The good superconductivity of the latter is obtained by doping extra electrons from Li atoms into binary hydrides MgH$_{16}$, breaking down the H molecules to atomic hydrogen [35].

Using the next lightest element, helium, may be another promising route in developing hydrogen superconductors. Despite helium being generally unreactive at ambient conditions, recent studies have reported weakly bonded van der Waals helium compounds (e.g., NH$_3$He [36], HeN$_4$ [37], HeFeO$_2$ [38], HeFe [39], HeH$_2$O [40,41], and Na$_2$He [42]). Compressing He and H, the two simplest and most abundant elements in the universe, is crucial to develop new condensed matter theories [15,43,44] and provide insights into the internal structure of the giant planets. For example, a new theory on the phase separation of H$_2$ and He shows that He can generate gravitational energy that drives planetary dynamics and contributes to the luminosity observed in Saturn [45]. Additionally, the miscibility of H with He or other planetary constitutes (H$_2$O, NH$_3$, and CH$_4$) can significantly affects to the physical properties, e.g., diffusivity and conductivity [36,40,46,47]. Recent experiment shows spectral evidence for mixtures of H$_2$ and He [48], however, it was later challenged by Raman spectroscopy that the reported chemical association is in fact from N$_2$ contamination [49]. These two conflict experiment results motivate the subsequent theoretical studies [50,51], which both exclude the existence of stable H-He compounds at high pressure based on the first-principle calculations. Very recently, another theoretical work proposed that He and H could form stable van der Waals compound (H$_2$)$_3$He below 8 GPa [52], while this structure is a wide gap insulator, indicating higher pressure is needed if we aim to obtain the metallic H-He compounds. Moreover, considering zero electronegativity of helium, it is interesting to know whether the intercalation of He atoms could facilitate the formations of new hydrogen motifs under extra high pressure, and if so, whether compounds are good superconductors.

Here, by performing a systematic structural search for H$_x$He ($x = 1$–12) at 800 GPa, we identify a dynamically stable hexagonal structure (h-H$_2$He), which displays an interesting metal hydrogen graphenelike motif. Electron-phonon calculations show this structure to exhibit weak superconductivity, which could be significantly enhanced by n-type

*wenwencui@jsnu.edu.cn
†yinwei_li@jsnu.edu.cn

doping. Our results are expected to guide the discovery of new metallic hydrogen motifs under high pressure with tunable superconductivity through electron doping.

II. COMPUTATIONAL DETAILS

Our search for binary H-He crystalline structures employs structural prediction up to four formula units using particle-swarm optimization algorithm (CALYPSO) [53–55]. CALYPSO is one of the most efficient methods for structural prediction and has successfully predicted stable or metastable ground-state structures for various systems at high pressure [16,19,23,24,56]. We have performed structure simulations for stoichiometries H_xHe ($x = 1$–12) with 1 to 4 formula at 800 GPa. In structure prediction runs, each generation contains 50 structures. More than 2000 structures were sampled for each prediction and the structure prediction can be stopped when another ~ 1000 structures were generated after finding the lowest-energy structure. The following structure relaxations and electronic properties are calculated using density functional theory implemented in VASP code [57]. The exchange-correlation potential is adopted for the generalized gradient approximation (GGA) [58] in the form of the Perdew-Burke-Ernzerhof (PBE) [59] functional. The all-electron projector augmented wave [58] method is used with valence electrons of $1s^1$ and $1s^2$ for H and He, respectively. The Monkhorst-Pack k-points [60] with a grid density of 0.2 Å^{-1} were chosen to make a total energy convergence of better than 1 meV per atom. The cutoff energy for the expansion of the wave function in the plane wave basis was set to 1000 eV. The electron-phonon coupling (EPC) for all structures were performed by using the linear response theory through QUANTUM-ESPRESSO code [61] with ultrasoft pseudopotentials and a kinetic cutoff energy of 100 Ry. The pseudopotentials were obtained from the PSlibrary (1.0 version) [62,63] using H $1s^1$ and He $1s^2$ valence electrons and the PBE exchange-correlation functional with cutoff radii of 0.75 and 0.6 for H and He, respectively. The q mesh of $4 \times 4 \times 2$ and k mesh of $16 \times 16 \times 8$ for the H_2He in the first Brillouin zone were used in the EPC calculations.

III. RESULTS AND DISCUSSION

On the basis of the predicted H_2-He solid structures, we indeed identify a group of H-He compounds (e.g., HHe, H_2He, H_3He, and H_5He), which contain interesting graphene-like hydrogen motifs (see Fig. 1 and Fig. S1 [64]), although they are energetically unstable with respect to elements with inclusion of zero-point energy (ZPE) (Figs. S2 and S3). Among these, H_2He is the only metallic compound with high symmetry, which is a general property in high-T_c superconductors [23,65]. For other different stoichiometries, we perform the same structural search to identify the best structure and all the structure parameters are shown in Tables S1 and S2. One can see that for hydrogen-rich H_xHe ($x \geqslant 4$) compounds, most of them adopt low symmetry $P1$, which is not favorable for possessing high-T_c superconductivity. Thus, hereafter the discussions will focus on the H_2He, which may show potential superconductivity.
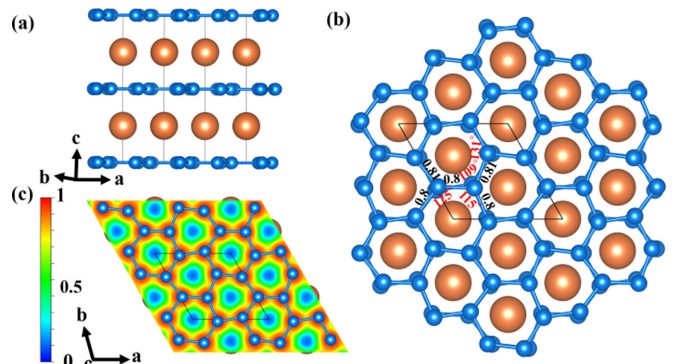

FIG. 1. (a) and (b) are structural configurations of $P\bar{6}$ phase of H_2He at 800 GPa in side and top view, respectively. (c) Two dimensional ELF of $P\bar{6}$ phase of H_2He. The small blue and large orange spheres represent H and He atoms, respectively.

H_2He was previously reported to be dynamically unstable at ambient pressure [52], while we predict three candidate structures for H_2He adopting $P\bar{6}$, $Cmmm$ and $P6/mmm$ symmetry, among which $P\bar{6}$ is the most stable structure (Fig. S3). Moreover, $P6/mmm$ is dynamically unstable with imaginary frequencies in phonon dispersions (Fig. S4), thus we choose the $P\bar{6}$ phase as a representative to investigate the electronic properties of H_2He. This novel phase of H_2He with $P\bar{6}$ symmetry displays a distorted well-known MgB$_2$ structure [66], namely, comprising alternating H and He layers [Fig. 1(a)], where the H atoms form a graphenelike sublattice [Fig. 1(b)]. However, unlike graphene, the H-H distances in the honeycomb slightly vary between 0.8 and 0.81 Å, thus distorting the hexagons [Fig. 1(b)]. The H-H distance is slightly elongated compared with that in pure solid H$_2$ (0.74 Å) and the strong covalent bonding between two H atoms is evidenced by the electron localization function (ELF) [Fig. 1(c)]. Note that a metastable phase in LiH$_2$ [67] is proposed to adopt the same structure as MgB$_2$ [66], however, the H-H distance (1.16 Å at 800 GPa) in the H layer is too long to form a covalent bond. In fact, pure solid hydrogen displays pronounced layerlike characters and graphene layers emerge in some metastable structures in solid hydrogen at high pressure [68].

Previous studies have demonstrated that two criteria have to be satisfied for finding higher-T_c BCS superconductors in highly compressed hydrides: (i) A large total DOS at Fermi level (E_f), and (ii) a high contribution of H-derived DOS. Distinctive features of hydrides are the transparency of the mechanism of their superconductivity, and close agreement between predictions and experiments [3]. We assume that the H_2He is a typical BCS superconductor, whose superconductivity could be theoretically well described. In order to investigate the superconductive potential of H_2He, we first calculated its electronic band structures and DOS [Fig. 2(a)]. The weak metallic features are revealed by only a few bands crossing E_f and also confirmed by the low occupation at the E_f (0.055 eV^{-1} per cell), which obviously violates criteria (i). However, H atoms dominating the total DOS which satisfies criteria (ii) indicates possible high superconductivity if the total DOS at the E_f can be greatly increased by adding extra electrons.
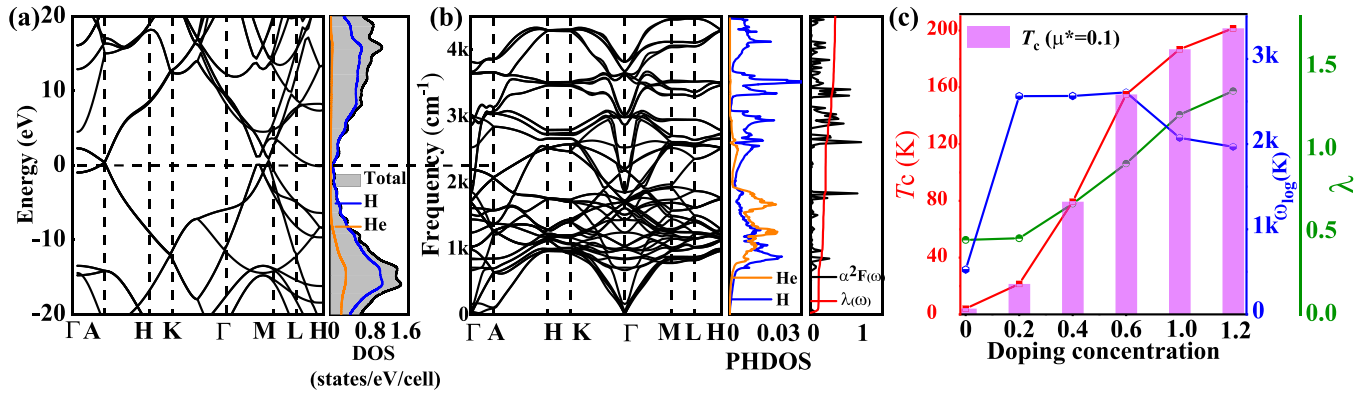
FIG. 2. (a) Calculated electronic band structure of $P\bar{6}$ H_2He. (b) Phonon dispersions, projected phonon density of states (PHDOS), Eliashberg spectral function $\alpha^2F(\omega)$, and electron-phonon coupling parameter λ of $P\bar{6}$ H_2He. (c) The calculated T_c logarithmic average phonon frequency ω_{log} and λ with respect to dopant concentration.

The dynamic stability of pristine H_2He is evidenced by absence of any imaginary frequencies [Fig. 2(b)]. The vibration modes of pristine structure [Fig. 2(b)] are easily divided into two parts: Below 2000 cm^{-1}, hybrid vibrations originate from H and He atoms, whereas at 2000-4500 cm^{-1}, there are almost exclusively vibrations of the H atoms. To investigate the structure's superconductivity, we calculate Eliashberg spectral function $\alpha^2F(\omega)$ and integrated EPC strength $\lambda(\omega)$. The resulting EPC parameter λ is 0.44 and the high-frequencies (> 2000 cm^{-1}), derived from combinational vibration of H-bending and stretching modes, contribute about 39% to the total λ. We use a typical value of Coulomb pseudopotential $\mu^* = 0.1$ to estimate the T_c value by using Allen-Dynes modified McMillian equation [69], yielding a total $T_c = 4$ K. The weak superconductivity is understandable, considering the low DOS occupation at E_f.

Electron doping can raise T_c evidenced by several studies [70–73] with the extra electrons being compensated by a uniform neutralizing background using a jellium model [74–78]. It is interesting and promising that the effect of doping on the EPC-driven superconductivity is expanded to be applicable to recently discovered hydrides under high pressure [3]. For example, the T_c could be significantly increased from 84 K to 148 K in CeH_9 by 0.3 hole doping [79]. Another example is FeH_5 [71], which exhibits no superconductivity in pristine structure and becomes a superconductor through different concentrations of electron doping, with the maximum T_c of 40 K by 0.5 e doping. We thus attempt to use n-type doping to improve the superconductivity of H_2He if an extra electron can be mainly attracted by H atoms, which could satisfy the criteria (ii).

As expected, the superconductivity is significantly enhanced by electron doping [Fig. 2(c)], which is greatest (201 K) in 1.2 e-doped H_2He. To clarify the origin of enhanced superconductivity, the modification of crystal structures, electronic properties, and electron-phonon coupling after doping will thus be discussed in detail below.

Crystal structures. Under different concentrations of electrons, both the lattice constants and atomic structures were fully relaxed. The structure maintains its $P\bar{6}$ symmetry after adding 0.2 e [Fig. S5(a)], but more electrons (0.4–1.2 e)

lead to a lower-symmetry Pm structure [Figs. S5(b)-(e)] after full structural relaxation. The average length of H-H bond lengths is slightly elongated from 0.81 Å (pristine structure) to 0.85 Å (1.2 e-doped structure), which can be attributed to the accepted extra electron. This is quite normal in compressed hydrides [19,23,24], where the transferred charge resides in the H_2 antibonding orbital, and thus lengthens the intramolecular bond.

Electronic properties. Figures 3(a)–3(c) show the electronic band structures of H_2He when doping electrons with values of 0.2, 0.6, and 1.2 e, respectively. As expected, the DOS at E_f correspondingly increases with increasing electron doping as compared with pristine structure (0.055 eV^{-1} per cell), namely, 0.12, 0.33, and 0.36 eV^{-1} per cell for 0.2, 0.6, and 1.2 e doping, respectively. Moreover, similar to pristine structure [Fig. 2(a)], the DOS occupations at E_f are dominated by H atoms, but with much larger values. The higher the value, the greater the possibility of the formation of Cooper pairs that may contribute to enhance T_c. For 0.2 e doping [Fig. 3(a)], E_f is shifted upward as compared to pristine band structure [Fig. 2(a)], and the higher doping levels due to the structural distortion alter the overall band structure as several bands emerge along the A-K direction and disappear along the M-L direction at E_f [Figs. 3(b) and 3(c)].

Electron-phonon coupling. For the doped structures, the frequencies are also divided into two parts with boundary at 2000 cm^{-1} [Fig. 4(a)-4(b) and Fig. S6], analogous to that of pristine structure. However, the resulting λ values are gradually increased with increasing doping [Fig. 2(c)], especially in the 1.2 e-doped structure, whose λ is up to 1.35, triple that of pristine H_2He (0.44). Two distinct peaks at 1300 and 2000 cm^{-1}, as highlighted by the gray area in Fig. 4(c), lead to a pronounced increase of λ, which arise from H-stretching and bending modes. Note that the contribution to the λ from the vibrations of H atoms exclusively (>2000 cm^{-1}) exceeds 50% in all the doped structure, which is substantially larger than that of pristine structure (39%). The combined increases λ and PDOS of H atoms at E_f significantly enhanced T_c [Fig. 2(c)], which is greatest (201 K) in 1.2 e-doped H_2He. When we continue to increase the doping electron to 1.5 e, the structure is dynamically unstable [Fig. S6(d)], which indicates that it is not accessible to dope too many electrons in H_2He.
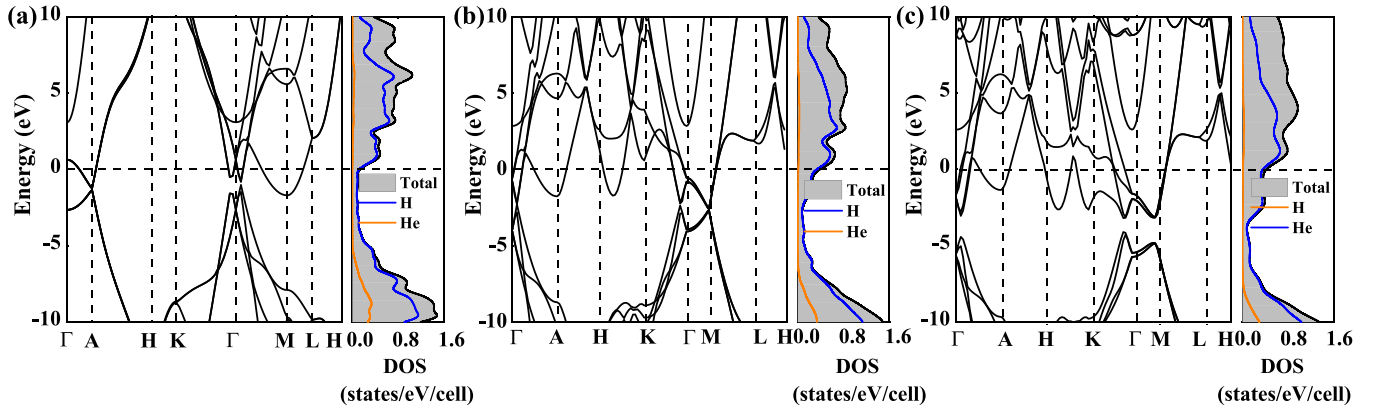
FIG. 3. Calculated electronic band structure of $P\bar{6}$ H$_2$He for (a) doping 0.2 electrons, (b) 0.6 electrons, and (c) 1.2 electrons.

When replacing freely rotating molecules in hydrogen-IV with He, Xe, and Ne atoms, we obtain the same $P6/mmm$ symmetry. For H$_2$Xe, previous study predicted that $Cmcm$ is the only energetically stable phase below 300 GPa [80], we thus calculated the enthalpies of these two phases as a function of pressure [Fig. S7(a)] and found that $Cmcm$ is still the most stable phase even at high pressure. Additionally, it is a superconductor with a maximum T_c of 26 K at 400 GPa and decreases with increasing pressure [80], while this phase only contains H$_2$ molecules [Fig. S7(b)]. It is not surprising that Xe could form stable hydrides at high pressure, since it is the most chemically active noble gas, while $P6/mmm$ H$_2$Ne is energetically unstable respective to elements just like He. Additionally, it is dynamically unstable with displaying imaginary phonon frequencies (Fig. S8), which is not under our consideration any more.

Transition metal atoms have diverse d electron configurations, which can be used as the electron donors. A further investigation used electron-donating transition metals Sc and Ti as substitutes for He atoms. The space group of the H$_2$Sc and H$_2$Ti structure evolves to $P6/mmm$ (the isostructure of MgB$_2$), and the H-H distance in the graphenelike hexagons have the same length of 1.22 Å (Fig. S9). Interestingly, the $P6/mmm$ H$_2$Sc has been previously proposed to possess T_c of 4 K at 300 GPa [81]. While for H$_2$Ti, the $Cmma$ phase is stable above 78 GPa, with T_c of 5.7 K at 250 GPa [82].

We then calculated the relative enthalpy of H$_2$Ti for these two phases and found that $P6/mmm$ phase is stable above 480 GPa (Fig. S10). Bader analysis shows that both Sc and Ti atoms will transfer about 0.5 electron to the graphene H. Compared with H$_2$He, both H$_2$Sc and H$_2$Ti have greater total DOS at E_f, however, the contribution of H atoms to the DOS occupations are negligible (Fig. S11), which fails to fit the criteria (ii), thus only increases the superconducting temperature of Sc and Ti replacing H$_2$He from 4 K to about 10 K (Fig. S12). These results further demonstrate the necessity of two criteria for attaining high-T_c superconductors.

IV. CONCLUSIONS

In summary, our extensive first-principle structural searches for the H-He system under high pressure have identified a metastable h-H$_2$He structure. This structure adopts a distorted MgB$_2$ structure, comprising alternating hexagonal hydrogen layers and He layers. Further electron-phonon calculations demonstrate the H$_2$He exhibits weak superconductivity due to the low DOS at E_f, which can be effectively tuned through n-type doping. T_c can be significantly enhanced to 155 and 201 K for doping 0.6 and 1.2 e, respectively, where the high-T_c superconductivity originates from synergetic effects of increased H-derived DOS at E_f and electron-phonon coupling related to the vibration modes of H atoms. Our
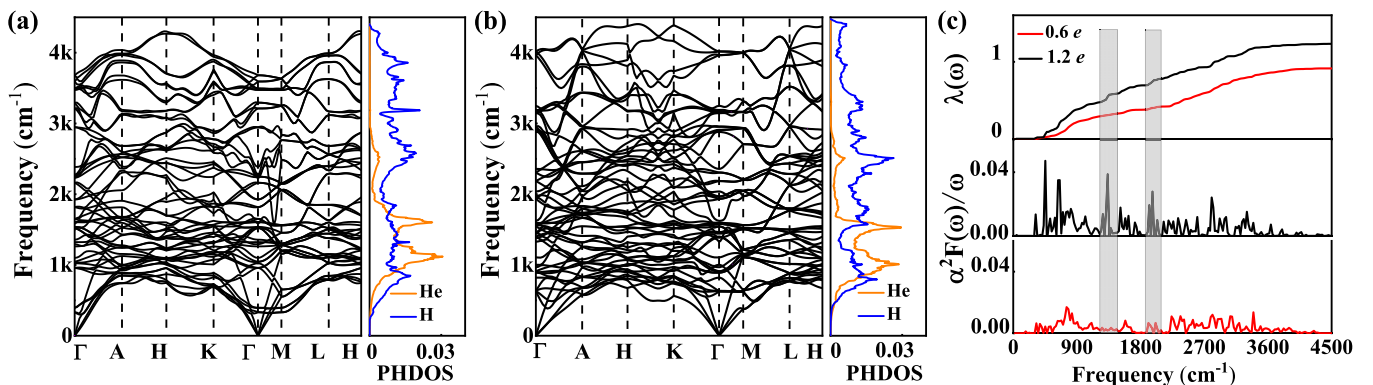

FIG. 4. Phonon dispersions and PHDOS of $P\bar{6}$ H$_2$He (a) with doping 0.6 electrons, (b) with doping 1.2 electrons. (c) Shows Eliashberg spectral function $\alpha^2F(\omega)/\omega$ and λ for different dopant concentration. Shaded regions in (c) show the significant contribution of two strong peaks of $\alpha^2F(\omega)/\omega$ to λ.

findings suggest that high pressure can lead to exotic hydrogen motifs in hydrides, whose superconductivity is tunable by electron doping.

ACKNOWLEDGMENTS

[1] E. Zurek and T. Bi, J. Chem. Phys. **150**, 050901 (2019).

[2] D. V. Semenok, I. A. Kruglov, I. A. Savkin, A. G. Kvashnin, and A. R. Oganov, Curr. Opin. Solid State Mater. Sci. **24**, 100808 (2020), and references therein.

[3] J. A. Flores-Livas, L. Boeri, A. Sanna, G. Profeta, R. Arita, and M. Eremets, Phys. Rep. **856**, 1 (2020).

[4] J. Lv, Y. Sun, H. Liu, and Y. Ma, Appl. Matter Radiat. Extremes **5**, 068101 (2020).

[5] W. Cui and Y. Li, Chin. Phys. B **28**, 107104 (2019).

[6] D. van Delft and P. Kes, Phys. Today **63**, 38 (2010).

[7] J. Bardeen, L. N. Cooper, and J. R. Schrieffer, Phys. Rev. **108**, 1175 (1957).

[8] N. W. Ashcroft, Phys. Rev. Lett. **21**, 1748 (1968).

[9] S. A. Bonev, E. Schwegler, T. Ogitsu, and G. Galli, Nature (London) **431**, 669 (2004).

[10] J. McMinis, R. C. Clay III, D. Lee, and M. A. Morales, Phys. Rev. Lett. **114**, 105305 (2015).

[11] J. M. McMahon and D. M. Ceperley, Phys. Rev. Lett. **106**, 165302 (2011).

[12] E. Wigner and H. á. Huntington, J. Chem. Phys. **3**, 764 (1935).

[13] S. Azadi, B. Monserrat, W. M. C. Foulkes, and R. J. Needs, Phys. Rev. Lett. **112**, 165501 (2014).

[14] R. P. Dias and I. F. Silvera, Science **355**, 715 (2017).

[15] N. W. Ashcroft, Phys. Rev. Lett. **92**, 187002 (2004).

[16] Y. Li, J. Hao, H. Liu, Y. Li, and Y. Ma, J. Chem. Phys. **140**, 174712 (2014).

[17] D. Duan, Y. Liu, F. Tian, D. Li, X. Huang, Z. Zhao, H. Yu, B. Liu, W. Tian, and T. Cui, Sci. Rep. **4**, 6968 (2015).

[18] A. Drozdov, M. Eremets, I. Troyan, V. Ksenofontov, and S. I. Shylin, Nature (London) **525**, 73 (2015).

[19] H. Liu, I. I. Naumov, R. Hoffmann, N. Ashcroft, and R. J. Hemley, Proc. Natl. Acad. Sci. USA **114**, 6990 (2017).

[20] M. Kostrzewa, K. Szczęśniak, A. Durajski, and R. Szczęśniak, Sci. Rep. **10**, 1592 (2020).

[21] A. Drozdov, P. Kong, V. Minkov, S. Besedin, M. Kuzovnikov, S. Mozaffari, L. Balicas, F. Balakirev, D. Graf, V. Prakapenka *et al.*, Nature (London) **569**, 528 (2019).

[22] M. Somayazulu, M. Ahart, A. K. Mishra, Z. M. Geballe, M. Baldini, Y. Meng, V. V. Struzhkin, and R. J. Hemley, Phys. Rev. Lett. **122**, 027001 (2019).

[23] F. Peng, Y. Sun, C. J. Pickard, R. J. Needs, Q. Wu, and Y. Ma, Phys. Rev. Lett. **119**, 107001 (2017).

[24] Y. Li, J. Hao, H. Liu, S. T. John, Y. Wang, and Y. Ma, Sci. Rep. **5**, 9948 (2015).

[25] P. Kong, V. S. Minkov, M. A. Kuzovnikov, A. P. Drozdov, S. P. Besedin, S. Mozaffari, L. Balicas, F. F. Balakirev, V. B. Prakapenka, S. Chariton, D. A. Knyazev, E. Greenberg, and M. I. Eremets, Nat. Commun. **12**, 5075 (2021).

[26] I. A. Troyan, D. V. Semenok, A. G. Kvashnin, A. V. Sadakov, O. A. Sobolevskiy, V. M. Pudalov, A. G. Ivanova, V. B. Prakapenka, E. Greenberg, A. G. Gavriliuk *et al.*, Adv. Mater. **33**, 2006832 (2021).

[27] E. Snider, N. Dasenbrock-Gammon, R. McBride, X. Wang, N. Meyers, K. V. Lawler, E. Zurek, A. Salamat, and R. P. Dias, Phys. Rev. Lett. **126**, 117003 (2021).

[28] W. Chen, D. V. Semenok, X. Huang, H. Shu, X. Li, D. Duan, T. Cui, and A. R. Oganov, Phys. Rev. Lett. **127**, 117001 (2021).

[29] N. P. Salke, M. M. D. Esfahani, Y. Zhang, I. A. Kruglov, J. Zhou, Y. Wang, E. Greenberg, V. B. Prakapenka, J. Liu, A. R. Oganov *et al.*, Nat. Commun. **10**, 4453 (2019).

[30] H. Wang, S. T. John, K. Tanaka, T. Iitaka, and Y. Ma, Proc. Natl. Acad. Sci. USA **109**, 6463 (2012).

[31] L. Ma, K. Wang, Y. Xie, X. Yang, Y. Wang, M. Zhou, H. Liu, X. Yu, Y. Zhao, H. Wang, G. Liu, and Y. Ma, Phys. Rev. Lett. **128**, 167001 (2022).

[32] Z. Li, X. He, C. Zhang, X. Wang, S. Zhang, Y. Jia, S. Feng, K. Lu, J. Zhao, J. Zhang, B. Min, Y. Long, R. Yu, L. Wang, M. Ye, Z. Zhang, V. Prakapenka, S. Chariton, P. A. Ginsberg, J. Bass *et al.*, Nat. Commun. **13**, 2863 (2022).

[33] K. Gao, W. Cui, J. Chen, Q. Wang, J. Hao, J. Shi, C. Liu, S. Botti, M. A. L. Marques, and Y. Li, Phys. Rev. B **104**, 214511 (2021).

[34] X. Feng, J. Zhang, G. Gao, H. Liu, and H. Wang, RSC Adv. **5**, 59292 (2015).

[35] Y. Sun, J. Lv, Y. Xie, H. Liu, and Y. Ma, Phys. Rev. Lett. **123**, 097001 (2019).

[36] J. Shi, W. Cui, J. Hao, M. Xu, X. Wang, and Y. Li, Nat. Commun. **11**, 3164 (2020).

[37] Y. Li, X. Feng, H. Liu, J. Hao, S. A. Redfern, W. Lei, D. Liu, and Y. Ma, Nat. Commun. **9**, 722 (2018).

[38] J. Zhang, J. Lv, H. Li, X. Feng, C. Lu, S. A. T. Redfern, H. Liu, C. Chen, and Y. Ma, Phys. Rev. Lett. **121**, 255703 (2018).

[39] B. Monserrat, M. Martinez-Canales, R. J. Needs, and C. J. Pickard, Phys. Rev. Lett. **121**, 015301 (2018).

[40] C. Liu, H. Gao, Y. Wang, R. J. Needs, C. J. Pickard, J. Sun, H.-T. Wang, and D. Xing, Nat. Phys. **15**, 1065 (2019).

[41] H. Liu, Y. Yao, and D. D. Klug, Phys. Rev. B **91**, 014102 (2015).

[42] X. Dong, A. R. Oganov, A. F. Goncharov, E. Stavrou, S. Lobanov, G. Saleh, G.-R. Qian, Q. Zhu, C. Gatti, V. L. Deringer *et al.*, Nat. Chem. **9**, 440 (2017).

[43] J. M. McMahon, M. A. Morales, C. Pierleoni, and D. M. Ceperley, Rev. Mod. Phys. **84**, 1607 (2012).

[44] C. J. Pickard, M. Martinez-Canales, and R. J. Needs, Phys. Rev. B **85**, 214114 (2012).

[45] J. J. Fortney and W. Hubbard, Astrophys. J. **608**, 1039 (2004).

[46] H. Gao, C. Liu, A. Hermann, R. J. Needs, C. J. Pickard, H.-T. Wang, D. Xing, and J. Sun, Natl. Sci. Rev. **7**, 1540 (2020).

[47] P. Huang, H. Liu, J. Lv, Q. Li, C. Long, Y. Wang, C. Chen, R. J. Hemley, and Y. Ma, Proc. Natl. Acad. Sci. USA **117**, 5638 (2020).

[48] J. Lim and C.-S. Yoo, Phys. Rev. Lett. **120**, 165301 (2018).

[49] R. Turnbull, M.-E. Donnelly, M. Wang, M. Peña-Alvarez, C. Ji, P. Dalladay-Simpson, H.-k. Mao, E. Gregoryanz, and R. T. Howie, Phys. Rev. Lett. **121**, 195702 (2018).

[50] X. Jiang, Y. Zheng, X.-X. Xue, J. Dai, and Y. Feng, J. Chem. Phys. **152**, 074701 (2020).

[51] S. B. Ramsey, M. Pena-Alvarez, and G. J. Ackland, Phys. Rev. B **101**, 214306 (2020).

[52] A. O. Adeniyi, A. A. Adeleke, X. Li, H. Liu, and Y. Yao, Phys. Rev. B **104**, 024101 (2021).

[53] Y. Wang, J. Lv, L. Zhu, and Y. Ma, Phys. Rev. B **82**, 094116 (2010).

[54] Y. Wang, J. Lv, L. Zhu, and Y. Ma, Comput. Phys. Commun. **183**, 2063 (2012).

[55] B. Gao, P. Gao, S. Lu, J. Lv, Y. Wang, and Y. Ma, Sci. Bull. **64**, 301 (2019).

[56] W. Cui, T. Bi, J. Shi, Y. Li, H. Liu, E. Zurek, and R. J. Hemley, Phys. Rev. B **101**, 134504 (2020).

[57] G. Kresse and J. Furthmüller, Phys. Rev. B **54**, 11169 (1996).

[58] A. V. dos Santos, G. Padilha, and M. Monçalves, Solid State Sci. **14**, 269 (2012).

[59] P. E. Blöchl, O. Jepsen, and O. K. Andersen, Phys. Rev. B **49**, 16223 (1994).

[60] H. J. Monkhorst and J. D. Pack, Phys. Rev. B **13**, 5188 (1976).

[61] P. Giannozzi, S. Baroni, N. Bonini, M. Calandra, R. Car, C. Cavazzoni, D. Ceresoli, G. L. Chiarotti, M. Cococcioni, I. Dabo *et al.*, J. Phys.: Condens. Matter **21**, 395502 (2009).

[62] A. Dal Corso, Comput. Mater. Sci. **95**, 337 (2014).

[63] K. Lejaeghere, G. Bihlmayer, T. Björkman, P. Blaha, S. Blügel, V. Blum, D. Caliste, I. E. Castelli, S. J. Clark, A. Dal Corso *et al.*, Science **351**, aad3000 (2016).

[64] See Supplemental Material at http://link.aps.org/supplemental/10.1103/PhysRevB.107.024501. It contains the convexhull of H-He compounds at 800 GPa, crystal structures of other H-He compounds, the structural information of pristine and doped H_2He. The calculated electronic band structures of TiH_2 and ScH_2, etc.

[65] L. Zhang, Y. Wang, J. Lv, and Y. Ma, Nat. Rev. Mater. **2**, 17005 (2017).

[66] J. Nagamatsu, N. Nakagawa, T. Muranaka, Y. Zenitani, and J. Akimitsu, Nature (London) **410**, 63 (2001).

[67] A. M. Shipley, M. J. Hutcheon, R. J. Needs, and C. J. Pickard, Phys. Rev. B **104**, 054501 (2021).

[68] C. J. Pickard and R. J. Needs, Nat. Phys. **3**, 473 (2007).

[69] P. B. Allen and R. Dynes, Phys. Rev. B **12**, 905 (1975).

[70] E. Sun, P. Zhang, H. Wang, H. Liu, and G. Liu, Phys. Lett. A, **402** 127348 (2021).

[71] C. Heil, G. B. Bachelet, and L. Boeri, Phys. Rev. B **97**, 214510 (2018).

[72] R. Xiao, D. Shao, W. Lu, H. Lv, J. Li, and Y. Sun, Appl. Phys. Lett. **109**, 122604 (2016).

[73] G. Savini, A. C. Ferrari, and F. Giustino, Phys. Rev. Lett. **105**, 037002 (2010).

[74] C. Si, Z. Liu, W. Duan, and F. Liu, Phys. Rev. Lett. **111**, 196802 (2013).

[75] D. Shao, W. Lu, H. Lv, and Y. Sun, Europhys. Lett. **108**, 67004 (2014).

[76] X. Xi, H. Berger, L. Forró, J. Shan, and K. F. Mak, Phys. Rev. Lett. **117**, 106801 (2016).

[77] G. Makov and M. C. Payne, Phys. Rev. B **51**, 4014 (1995).

[78] E. R. Margine and F. Giustino, Phys. Rev. B **90**, 014518 (2014).

[79] C. Wang, S. Liu, H. Jeon, S. Yi, Y. Bang, and J. H. Cho, Phys. Rev. B **104**, L020504 (2021).

[80] X. Yan, Y. Chen, X. Kuang, and S. Xiang, J. Chem. Phys. **143**, 124310 (2015).

[81] X. Ye, R. Hoffmann, and N. W. Ashcroft, J. Phys. Chem. C **119**, 5614 (2015).

[82] J. Zhang, J. M. Mcmahon, A. R. Oganov, X. Li, X. Dong, H. Dong, and S. Wang, Phys. Rev. B **101**, 134108 (2020).